JACS
JOURNAL OF THE AMERICAN CHEMICAL SOCIETY

Article

pubs.acs.org/JACS

Connectosomes for Direct Molecular Delivery to the Cellular Cytoplasm

Avinash K. Gadok,[†] David J. Busch,[†] Silvia Ferrati,[†,‡] Brian Li,[†] Hugh D. C. Smyth,[‡] and Jeanne C. Stachowiak*[,†,§]

[†]Department of Biomedical Engineering, [‡]College of Pharmacy, and [§]Institute for Cellular and Molecular Biology, The University of Texas at Austin, Austin, Texas 78712, United States

Supporting Information

ABSTRACT: Transport of biomolecules, drugs, and other reagents across the cell's plasma membrane barrier is an inefficient and poorly controlled process, despite its fundamental importance to biotechnology, cell biology, and pharmaceutics. In particular, insufficient membrane permeability frequently limits the accumulation of drugs and reagents in the cytoplasm, undermining their efficacy. While encapsulating drugs in particles increases uptake by cells, inefficient release of drugs from these particles into the cytoplasm ultimately limits drug efficacy. In contrast, gap junctions provide a direct route to the cytoplasm that bypasses the plasma membrane. As transmembrane channels that physically connect the cytoplasm of adjacent cells, gap junctions permit transport of a diverse range of molecules, from ions and metabolites to siRNA, peptides, and chemotherapeutics. To utilize gap junctions for molecular delivery we have developed Connectosomes, cell-derived lipid vesicles that contain functional gap junction channels and encapsulate molecular cargos. Here we show that these vesicles form gap junction channels with cells, opening a direct and efficient route for the delivery of molecular cargo to the cellular cytoplasm. Specifically, we demonstrate that using gap junctions to deliver the chemotherapeutic doxorubicin reduces the therapeutically effective dose of the drug by more than an order of magnitude. Delivering drugs through gap junctions has the potential to boost the effectiveness of existing drugs such as chemotherapeutics, while simultaneously enabling the delivery of membrane-impermeable drugs and reagents.

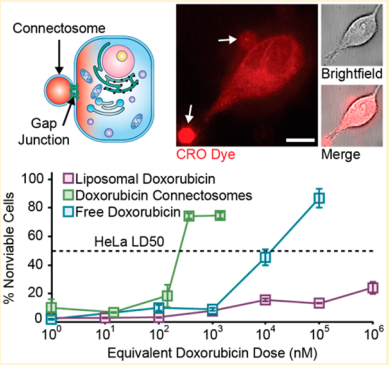

INTRODUCTION

Membrane permeability is a fundamental requirement for biomolecules, drugs, and reagents that act on intracellular targets. To cross the plasma membrane, molecules must be soluble in both the hydrophobic membrane environment and in the aqueous cytosol.[1] Meeting these requirements while maintaining activity frequently overconstrains molecular design. For example, the effectiveness of chemotherapeutic drugs with marginal membrane permeability, such as gemcitabine, cytarabine,[2] or cisplatin,[3] is limited by poor accumulation in the cytoplasm. Even highly membrane permeable drugs, such as doxorubicin,[4] have limited transport rates across the plasma membrane,[5] such that therapeutically effective doses are large, promoting systemic toxicity.[6] Further, increasing the membrane permeability of drugs also frequently increases their vulnerability to export by multidrug efflux pumps,[7] restricting their accumulation in the cytoplasm. In sum, crossing the plasma membrane is a substantial challenge that limits the performance of even the most successful drugs. This challenge is among the primary reasons that easily accessible cell-surface proteins, such as G-protein coupled receptors and ion channels, are the targets of the majority of existing drugs,[8] while many potentially valuable intracellular targets have not been successfully exploited.[9]

Toward overcoming the challenge of crossing the plasma membrane, drugs are frequently encapsulated within nanoparticle materials.[10,11] Loading doxorubicin into liposomes was one of the earliest uses of nanoparticles for drug delivery. This approach substantially reduced the drug's systemic toxicity,[4] illustrating the potential of nanoparticles to improve drug delivery. However, upon reaching tumor cells, nanoparticles enter cells through endocytosis,[12] frequently becoming trapped in the endosomal lumen, which is topologically equivalent to the extracellular milieu.[13] Inefficient endosomal escape leads to nanoparticle degradation and export,[14] limiting the efficiency of cytoplasmic delivery[15] and increasing the drug concentration required to kill cancer cells.[16] For example, in *in vitro* studies the therapeutically effective dose, i.e., the median lethal dose (LD50), of doxorubicin increases by an order of magnitude when the drug is encapsulated within liposomes.[16]

To facilitate endosomal escape, several strategies have been developed that incorporate pH-sensitive polymers,[17] peptides,[18] and other compounds[19] into nanoparticles. These membrane-disrupting agents are activated by the acidic endosomal environment, leading to intracellular release of encapsulated drugs.[20] Along with other triggered-release strategies,[21] these

Received: May 20, 2016
Published: September 8, 2016

DOI: 10.1021/jacs.6b05191
J. Am. Chem. Soc. 2016, 138, 12833−12840

advancements have reduced the therapeutically effective dose of particle-encapsulated doxorubicin to concentrations equivalent to the free drug.[17,19−21] Further, in some cases, endosomal release strategies have helped to overcome multidrug efflux processes,[22] and coupling endosomal release to materials with high drug-carrying capacities, such as silica protocells[23,24] or laponite disks,[25] has further reduced the therapeutically effective dose of particle-encapsulated doxorubicin to levels below that of the free drug.

Despite these substantial advancements, delivery approaches that rely upon endocytosis to achieve intracellular release remain constrained by the difficulty of controlling the process,[26] and by the variability of the endosomal environment, which frequently limits release.[27,28] For example, more than 80% of mesoporous silica nanoparticles are exocytosed from cells after 6 h,[14] leaving a limited window of time for intracellular drug release. In addition, less than 2% of lipid nanoparticles taken up by endocytosis escape from the endosome within 6 h.[29] In light of these persistent limitations, a new delivery route that bypasses endocytic pathways entirely has the potential to dramatically improve therapeutic efficacy.

By providing direct access to the cytoplasm, the cellular gap junction network suggests a means of circumventing the plasma membrane barrier. Cells exchange molecular cargo including metabolites, second messengers, peptides,[30] and siRNA with their neighbors using gap junctions.[31] The proteins that form gap junctions, connexins, assemble into connexons. These hexameric pores are present on the cellular plasma membrane. When connexons from two neighboring cells meet, they form a complete gap junction channel, enabling molecules to move from the cytoplasm of one cell to the next by diffusing through the channel. Through a phenomenon known as the bystander effect, cells share drugs via gap junctions. This effect enables drug penetration in tumors[32] and promotes the efficacy of diverse chemotherapeutics, including doxorubicin,[33] etoposide,[33] paclitaxel,[33] gemcitabine,[34] and others.[35] Inspired by the ability of gap junctions to directly access the cytoplasm, here we report the development of Connectosomes, connexon-containing cell-derived lipid vesicle materials that form functional gap junctions with cells. Using these materials, we demonstrate gap junction-dependent delivery of molecular cargo into the cytoplasm. Our results indicate that this approach reduces the therapeutically effective dose (LD50) of doxorubicin by more than an order of magnitude in comparison to the free drug and by multiple orders of magnitude in comparison to liposomal doxorubicin. These results demonstrate the potential of gap junction-mediated intracellular delivery to enhance the effectiveness of diverse therapeutics.

RESULTS AND DISCUSSION

Connexons have previously been reconstituted in synthetic vesicles for basic biological studies, demonstrating formation of functional junctions between vesicles and cells.[36] However, these vesicles have not been pursued for therapeutic purposes, likely due to technical difficulties including (i) purifying sufficient quantities of transmembrane proteins, (ii) inserting the proteins into vesicles, and (iii) controlling their orientation in the membrane. To overcome these limitations, we used the process of plasma membrane blebbing to harvest Connectosomes directly from donor cells that overexpressed gap junctions. Plasma membrane blebs, also known as plasma membrane vesicles, form when attachments between the plasma membrane and the cytoskeleton are disrupted[37] during cellular processes including cell motility and cytokinesis[37] and maintain the directional insertion and function of transmembrane proteins.[38] Plasma membrane blebs have frequently been used as biophysical models and have recently emerged as potentially attractive materials for therapeutic applications.[39,40] Notably, exosomes, which are cell-derived vesicles released from cells by fusion of multivesicular bodies to the plasma membrane,[41] have also recently emerged as potential drug delivery vehicles.[42] Plasma membrane blebs and exosomes differ in several significant ways, including the membrane system they originate from, and the extent to which their transmembrane protein content can be controlled. Specifically, blebs are derived directly from the plasma membrane system, while exosomes are derived from the cell's endosomal membrane system. Since protein traffic to the plasma membrane is well understood, conventional protocols can be used to express proteins at the plasma membrane surface, resulting in their incorporation into blebs.[43] In contrast, understanding of how protein sorting in the endosomal system leads to selection of proteins by the exosomal pathway is still emerging,[41] making the incorporation of specific protein constituents in exosomes difficult to predict and control. Nonetheless, a recent report suggests that connexins may contribute to the ability of exosomes to transfer their native internal contents to cells.[44] While this study did not investigate the use of connexins to deliver drugs, these findings are consistent with the idea that cell-derived particles with well-controlled connexin expression could provide an effective new mode of drug delivery.

By extracting blebs from donor cells that overexpressed connexin 43 proteins with a C-terminal YFP modification (Cx43-YFP), we produced cell-derived lipid vesicle materials with embedded connexin 43-YFP (Figure 1a−e, Supporting Information Movie S1). Over 90% of these Connectosomes contained connexin 43-YFP at levels detectable by fluorescence imaging. The Connectosomes ranged in diameter from 4 to more than 20 μm, with an average diameter of 10 μm (Figure 1j). Notably, Connectosomes can be extruded to reduce their diameter to around 100 nm. Based on quantitative measurements of YFP fluorescence, we determined that the average Connectosome contained over 400,000 connexons, which cumulatively covered nearly 10% of the vesicle surface (Figure 1k).

To test the functionality of connexon channels embedded in Connectosomes, we examined the ability of the channels to open and close in the absence and presence of calcium. Specifically, it is well established that calcium causes unpaired connexons to close, obstructing the passage of molecules.[45−47] However, in the absence of calcium, connexons undergo a conformational change that causes them to open, allowing small molecules to diffuse through them.[45] We began by examining the ability of connexons to open upon calcium removal, releasing dye encapsulated within the Connectosomes. To load Connectosomes with the dye we treated the donor cells with calcein red-orange (CRO) acetomethoxy (AM) prior to extracting membrane blebs (Figure 1f−i, Supporting Information Movie S2). CRO AM diffuses freely across the plasma membrane. However, when the dye reaches the cytoplasm, intracellular esterases hydrolyze the acetomethoxy group. The resulting CRO dye molecule is membrane impermeable, trapped inside of the cell and permeable only to gap junctions (Figure 1f).[48] In the presence of calcium, the Connectosomes retained the CRO dye (Figure 2a, top).

DOI: 10.1021/jacs.6b05191
J. Am. Chem. Soc. 2016, 138, 12833−12840

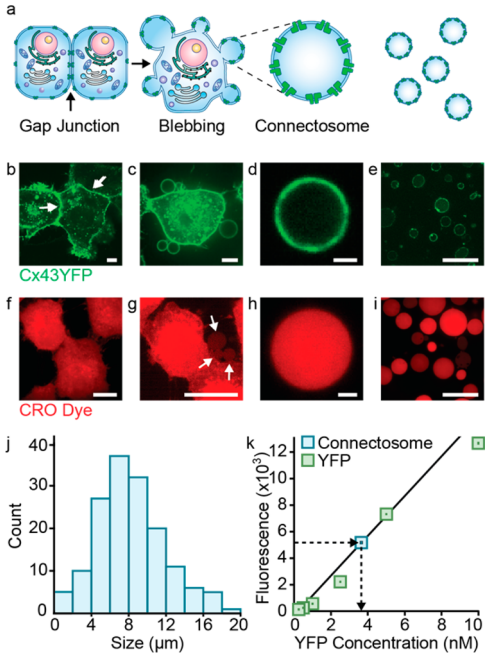

Figure 1. Connectosomes loaded with molecular cargo were harvested from donor cells. Confocal fluorescence images. (a) Schematic of the Connectosome production process. (b–d) Plasma membrane blebs were extracted from donor cells overexpressing connexin 43-YFP (arrows) to produce Connectosomes, cell-derived lipid vesicle materials with embedded connexin 43-YFP connexons. (e) Multiple Connectosomes in a single field of view. (f–h) Plasma membrane blebs (arrows) were extracted from donor cells treated with CRO dye to produce CRO dye-loaded Connectosomes. (i) Multiple CRO dye-loaded Connectosomes in a single field of view. (j) Histogram of Connectosome diameters. 154 Connectosomes were measured. (k) A calibration curve of YFP fluorescence was generated to determine the YFP content of the Connectosomes. All scale bars 20 μm except for (d) and (h), which are 2 μm. Images in (c) and (g) intentionally saturated to show Connectosome formation.

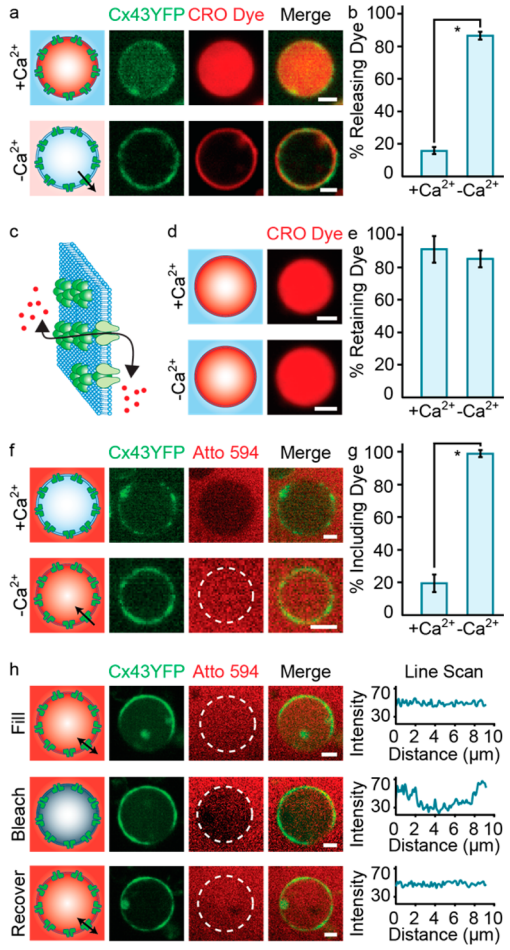

Figure 2. Connectosomes contained functional connexons. Confocal fluorescence images. (a) Connectosomes retained CRO dye in a solution of 2 mM Ca^{2+} (top) but released dye when Ca^{2+} was removed (bottom). (b) Percentage of Connectosomes releasing dye ± Ca^{2+}. The error bars represent the standard deviations of 3 independent trials; at least 54 Connectosomes analyzed per trial. (c) Schematic illustrating connexon-dependent molecular exchange. (d), Plasma membrane blebs derived from MDA-MB-231 cells retained CRO dye in a solution of 2 mM Ca^{2+} (top), as well as when Ca^{2+} was removed (bottom). (e) Percentage of MDA-MB-231 blebs releasing dye ± Ca^{2+}. The error bars represent the standard deviations of 3 independent trials, at least 36 Connectosomes analyzed per trial. (f) Connectosomes excluded Atto 594 in 2 mM Ca^{2+} (top) but filled with dye when Ca^{2+} was removed (bottom). (g) Percentage of Connectosomes including dye ± Ca^{2+}. The error bars represent the standard deviations of 3 independent trials, at least 51 Connectosomes analyzed per trial. (h) The Atto 594 dye within Connectosomes (top) was photobleached (middle) in the absence of Ca^{2+}. The Connectosomes refilled with dye within 75 s after the laser illumination was stopped (bottom). Scale bars: 2 μm. Asterisks represent statistically significant differences (two-tailed t test, $p < 0.001$).

However, when calcium was removed by addition of EGTA and EDTA chelators, the dye was released from 87% of the Connectosomes and retained by only 13%, demonstrating that the connexons opened (Figure 2a, bottom; b,c).

To further illustrate the dependence of dye release on the presence of functional connexons in the Connectosomes, we formed CRO dye-loaded plasma membrane blebs from MDA-MB-231 donor cells. MDA-MB-231 cells express low levels of connexin 43 and exhibit defective connexin trafficking and gap junction formation, resulting in substantially reduced gap junction intercellular communication.[49] In the presence of calcium, 91% of MDA-MB-231 blebs retained the dye (Figure 2d, top). When calcium was removed by addition of EGTA and EDTA chelators, 85% of the MDA-MB-231 blebs continued to retain the dye, in comparison to only 13% of Connectosomes, demonstrating that the dye release was dependent on the presence of functional connexons (Figure 2d, bottom; e).

Next, we developed an exogenous method of loading, in which molecular cargo was encapsulated after Connectosome formation. Specifically, we added a water-soluble dye with little or no membrane permeability, Atto 594, to the solution surrounding preformed Connectosomes. In the presence of calcium, the Connectosomes excluded the dye, demonstrating that connexons remained closed (Figure 2f, top). However, when calcium was removed by addition of EGTA and EDTA chelators, 99% of the Connectosomes filled with dye, demonstrating that the connexons opened (Figure 2f, bottom; g). Similar results were also obtained for Connectosomes loaded with Atto 488 dye using an identical protocol (Supporting Information Figure S1). Atto 488 has been reported to have no significant interaction with membranes,[50] making the dye almost perfectly membrane impermeable.

Finally, to probe the time scale of diffusion through open connexons, we photobleached Atto 594 dye loaded within the

DOI: 10.1021/jacs.6b05191
J. Am. Chem. Soc. 2016, 138, 12833–12840

Connectosomes. In the absence of calcium, the Connectosomes refilled with dye within 75 s after photobleaching (Figure 2h). Together, these results demonstrate two distinct modes of loading Connectosomes and demonstrate that Connectosomes contain multiple functional connexons, capable of opening and closing to enable rapid molecular exchange with the external environment. Further, comparison to MDA-MB-231 blebs suggests that molecular exchange is connexon-dependent.

Having established the functionality of the connexons, we next examined the ability of the Connectosomes to deliver molecular cargo into the cellular cytoplasm (Figure 3a). While

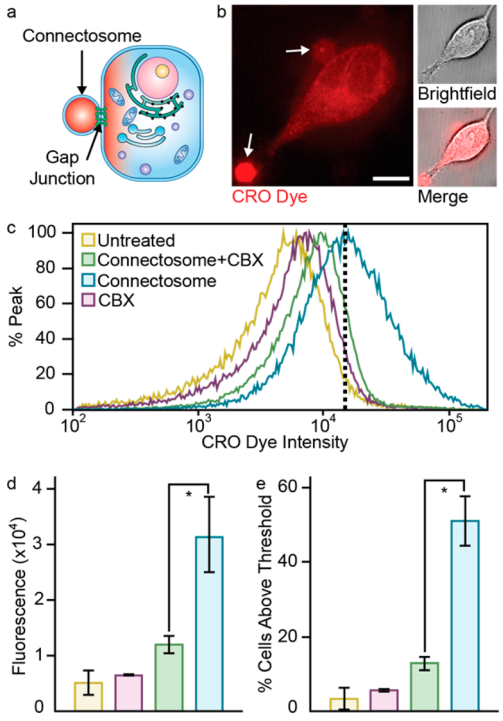

Figure 3. Connectosomes delivered dye to the cellular cytoplasm. Bright-field and confocal fluorescence images. (a) Schematic. (b) Two Connectosomes (arrows) delivering CRO dye to the cellular cytoplasm. (c) Flow cytometry histograms showing CRO dye fluorescence for each recipient cell condition. The dotted line, drawn at the peak of the fluorescence histogram for cells receiving CRO dye-loaded Connectosomes, is used as a threshold in (e). Each curve represents 3 independent, concatenated trials, 10 000 cells analyzed per trial. (d) Average recipient cell fluorescence for each condition. The error bars represent the standard deviations of 3 independent trials, 10 000 cells analyzed per trial. (e) Percentage of cells with fluorescence values above the threshold drawn in (c). The error bars represent the standard deviations of 3 independent trials, 10 000 cells analyzed per trial. Legend in (c) applies to (d, e). Scale bar: 10 μm. Asterisks represent statistically significant differences (two-tailed t test, $p < 0.04$ (d) and $p < 0.01$ (e)). Image of Connectosome in (b) intentionally saturated to show intracellular dye accumulation.

the presence of calcium keeps unpaired connexons closed,[45] complete channels form and open when two unpaired connexons on the surfaces of neighboring cells meet, even in the presence of physiological levels of extracellular calicium.[51,52] To test the ability of Connectosomes to form gap junctions with cells, we prepared a confluent monolayer of recipient HeLa cells. CRO dye-loaded Connectosomes were prepared as described above (Figure 1f–i) and incubated with the recipient cells. Imaging the recipient cells after 2 h revealed the intracellular accumulation of dye (Figure 3b, Supporting Information Figure S2). To quantify the CRO dye delivery, we measured the relative fluorescence intensity of the cell populations using flow cytometry (Figure 3c–e). Exposure to CRO dye-loaded Connectosomes increased the average fluorescence of the recipient cells by a factor of 6, in comparison to background fluorescence from untreated cells (Figure 3d, Supporting Information Figure S2). Additionally, we drew a threshold at the peak of the fluorescence histogram for cells receiving dye-loaded Connectosomes (Figure 3c). The average percentage of cells with fluorescence greater than this threshold increased from less than 4% for untreated cells to over 51% for cells exposed to dye-loaded Connectosomes (Figure 3e). To demonstrate that the CRO dye delivery was gap junction-dependent, we used carbenoxolone[53] (CBX), a drug which blocks the coupling of connexons, to inhibit the formation of gap junctions between Connectosomes and recipient HeLa cells. Repeating the dye delivery experiment in the presence of this gap junction inhibitor significantly decreased the average recipient cell fluorescence, illustrating that dye delivery was dependent on the assembly of gap junction channels between the Connectosomes and the cells (Figure 3c–e, Supporting Information Figure S2). CBX treatment did not completely eliminate the increase in fluorescence of the recipient cells upon exposure to dye-loaded Connectosomes, likely because CBX is not a complete inhibitor of gap junction communication[53] and because CBX itself somewhat increases the fluorescence of the recipient cells, in the absence of Connectosome treatment (Figure 3c–e, Supporting Information Figure S3).

To further demonstrate the gap junction dependence of the CRO dye delivery, we repeated the same experiment as above, using plasma membrane vesicles that lacked a significant concentration of functional connexons (Supporting Information Figure S4). Specifically, we formed CRO dye-loaded plasma membrane vesicles from A549 cells, which are known to have low levels of connexin expression and gap junctional communication.[54] We incubated these connexon-lacking plasma membrane vesicles with recipient HeLa cells and measured the relative recipient cell fluorescence using flow cytometry (Supporting Information Figure S4). We found that the fluorescence signal from cells exposed to CRO dye-loaded A549 vesicles was more than an order of magnitude less than the average fluorescence signal from cells exposed to Connectosomes. Collectively, these results demonstrate gap-junction-dependent delivery of molecular cargo using Connectosomes.

Next, we investigated the use of Connectosomes to deliver the chemotherapeutic doxorubicin to the cellular cytoplasm. We began with doxorubicin because its inherent fluorescence allowed us to visualize its encapsulation within Connectosomes. We note that doxorubicin may not be an ideal candidate for delivery via Connectosomes, owing to its cardiotoxicity and the importance of connexins in heart tissue. However, any small-molecule drug or biomolecule can in principle be encapsulated within Connectosomes, and nanoparticles in general have not been observed to accumulate in the heart.[55,56] Further, incorporation of targeting ligands has recently been demonstrated to dramatically increase binding specificity of cell-derived vesicles to target cells overexpressing biomarkers such as the epidermal growth factor receptor (EGFR).[57]

To encapsulate doxorubicin within Connectosomes, we treated donor cells with doxorubicin (Figure 4a), such that

DOI: 10.1021/jacs.6b05191
J. Am. Chem. Soc. 2016, 138, 12833–12840

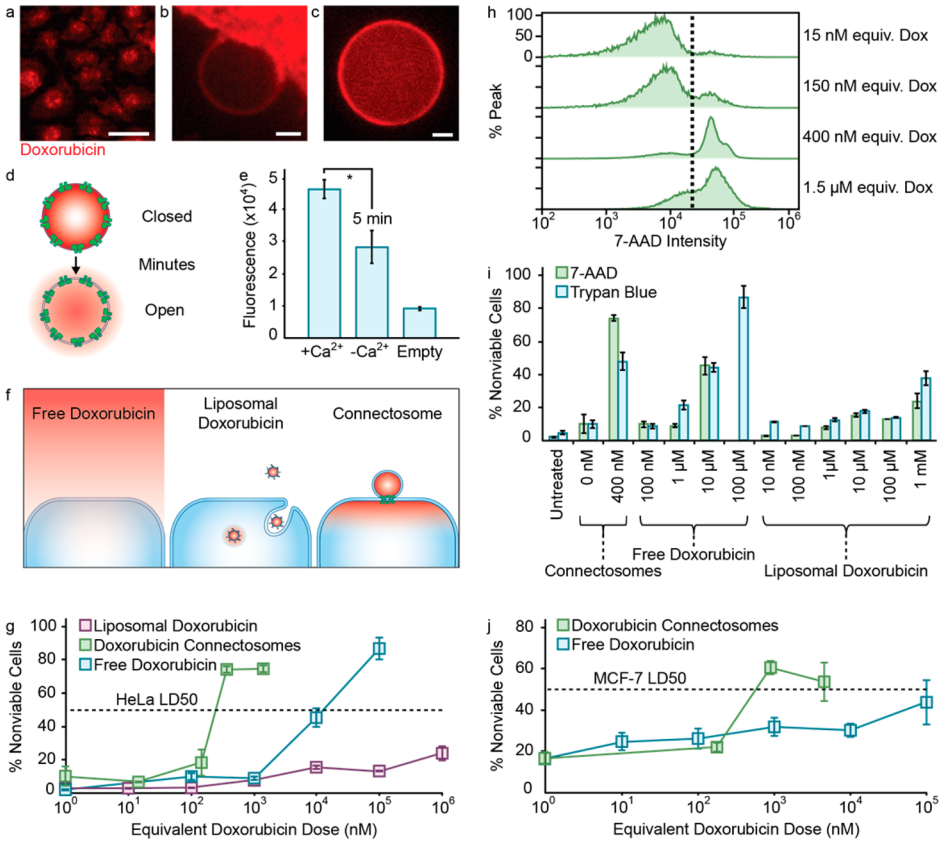

Figure 4. Connectosomes substantially reduced the cytotoxic dose of doxorubicin. (a–c) Plasma membrane blebs were extracted from donor cells treated with doxorubicin to produce doxorubicin-loaded Connectosomes. (d) Schematic illustrating doxorubicin release from Connectosomes. (e) Average Connectosome fluorescence calculated from flow cytometry data. Connectosomes released significant amounts of doxorubicin within 5 min of calcium removal. The error bars represent the standard deviations of 3 independent trials, at least 800 Connectosomes analyzed per trial. (f) Schematic illustrating the 3 modes of drug delivery tested. (g) Percentage of nonviable HeLa cells after free doxorubicin treatment (blue), conventional liposomal doxorubicin treatment (purple), or doxorubicin-loaded Connectosome treatment (green). All points were measured using a 7-AAD viability assay, except for the free doxorubicin 10^5 nM point, which was measured using a trypan blue viability assay, owing to interference of doxorubicin in the 7-AAD measurement at this high doxorubicin concentration. The error bars represent the standard deviations of at least 3 independent trials, at least 4000 cells (7-AAD assay) or 93 cells (trypan blue) analyzed per trial. (h) Flow cytometry histograms showing 7-AAD fluorescence for cells receiving doxorubicin-loaded Connectosomes at increasing equivalent free doxorubicin (dox) concentrations. The dotted line represents the threshold fluorescence value above which cells were considered nonviable. Each curve represents 3 independent, concatenated trials, at least 4000 cells analyzed per trial. (i) Percentage of nonviable cells determined using both trypan blue (blue) and 7-AAD (green) viability assays. The error bars represent the standard deviations of at least 3 independent trials, at least 4000 cells (7-AAD assay) or 93 cells (trypan blue assay) analyzed per trial. (j) Percentage of nonviable MCF-7 cells after free doxorubicin treatment (blue) or doxorubicin-loaded Connectosome treatment (green). All points were measured using a trypan blue viability assay. The error bars represent the standard deviations of 3 independent trials, at least 166 cells analyzed per trial. Scale bars: 2 μM. Asterisks represent statistically significant differences (two-tailed t test, $p < 0.02$). Image in (b) intentionally saturated to show doxorubicin-loaded Connectosome formation.

the plasma membrane blebs derived from these cells contained the drug (Figure 4b,c). Notably, chemotherapeutics such as doxorubicin require 2–3 days to substantially impact cell viability,[16] while harvesting Connectosomes requires only a few hours (see Methods, Supporting Information). Therefore, loss of donor cell viability owing to drug loading was found to be insignificant during the Connectosome production process. Additionally, it is important to note that doxorubicin could be encapsulated within Connectosomes either by loading the cells with the semimembrane permeable drug or by opening and subsequently closing the connexons of preformed Connectosomes in the presence of a solution of the drug. Loading of the cells prior to Connectosome extraction was found to slightly increase the concentration of encapsulated drug and the overall material yield (i.e., Connectosomes per donor cell) and was therefore used to produce the Connectosomes for the doxorubicin studies presented here.

We quantified the doxorubicin content of the Connectosomes by measuring their fluorescence emission after resuspending them in fresh solution (Supporting Information Figure S5). The native fluorescence of empty Connectosomes was measured and determined negligible. Based on the peak fluorescence emission of each Connectosome sample and a calibration curve of free doxorubicin fluorescence emission, we were able to determine that the average concentration of doxorubicin in each Connectosome sample was in the micromolar range. Based on this value as well as the average diameter and number of Connectosomes per volume, we estimated that the concentration of doxorubicin within Connectosomes was approximately 1 mM. Notably, this concentration could be further increased by crystallizing doxorubicin within vesicles, as is done in the preparation of conventional liposomal formulations.[4]

DOI: 10.1021/jacs.6b05191
J. Am. Chem. Soc. 2016, 138, 12833–12840

We then investigated the time scale of doxorubicin release from Connectosomes (Figure 4d). To begin, we measured the fluorescence of doxorubicin-loaded Connectosomes using flow cytometry (Figure 4e). After addition of EGTA and EDTA chelators to remove residual calcium and open connexons, the average doxorubicin fluorescence of the Connectosomes decreased significantly within 5 min. These results demonstrate the potential for rapid drug release upon connexon opening. In contrast, when chelators were not added, the vesicles retained their content throughout the time course of all experiments.

Next, we conducted a control study in which the viability of a confluent monolayer of HeLa cells was measured 24 h after free doxorubicin was added directly to the cell media at increasing concentrations from 100 nM to 100 μM (Figure 4f,g,i, Supporting Information Figure S6). The cytotoxic dose of doxorubicin for HeLa cells after 24 h of exposure is approximately 10 μM.[58] We evaluated cell viability using both trypan blue and 7-AAD cell permeability assays on at least 3 independent populations of cells per condition per stain. As expected, we found a trend of decreasing cell viability with increasing doxorubicin concentration. Specifically, while a dose of 100 nM was not significantly cytotoxic (9% trypan blue/10% 7-AAD), the percentage of nonviable cells increased with increasing doxorubicin dose at 1 μM (21% trypan blue/9% 7-AAD), 10 μM (44% trypan blue/45% 7-AAD), and 100 μM (87% trypan blue) (Figure 4g,i). Cells receiving 100 μM doxorubicin were outside the range of sensitivity for the 7-AAD assay; therefore, the percentage of nonviable cells at this concentration measured using the trypan blue assay was used in Figure 4g.

Then, we conducted a study in which the viability of a confluent monolayer of HeLa cells was measured 24 h after conventional, commercially sourced liposomal doxorubicin was added directly to the cell media at increasing doxorubicin concentrations from 10 nM to 1 mM (Figure 4f,g,i, Supporting Information Figure S6). These experimental parameters are consistent with the systemic infusions used to administer liposomal doxorubicin in the clinical setting. We evaluated cell viability using both trypan blue and 7-AAD cell permeability assays on at least 3 independent populations of cells per condition per stain. We found that the LD50 of liposomal doxorubicin was more than an order of magnitude greater than the LD50 of free doxorubicin (Figure 4g,i). This result confirms previous reports and likely arises from the inhibited release of doxorubicin when encapsulated within a liposome.[16]

Finally, we exposed confluent HeLa cell monolayers to doxorubicin-loaded Connectosomes for 2 h (Figure 4f). Independent cell samples were exposed to increasing concentrations of Connectosomes, which were equivalent in terms of total doxorubicin content to free doxorubicin concentrations of 15 nM, 150 nM, 400 nM, and 1.5 μM. As discussed above, these concentrations were determined by measuring the doxorubicin fluorescence emission for each sample (Supporting Information Figure S5). While the 15 nM Connectosome dose was not significantly cytotoxic (7% 7-AAD), the percentage of nonviable cells increased with increasing Connectosome concentration at 150 nM (18% 7-AAD), 400 nM (74% 7-AAD), and 1.5 μM (75% 7-AAD) (Figure 4g,h, Supporting Information Figure S7). To confirm our results, we repeated the experiment with doxorubicin-loaded Connectosomes at the lowest effective dose, 400 nM, measuring viability using the trypan blue assay (Figure 4i). The results of this study were comparable to the results of the 7-AAD assay.

To test Connectosomes in a second model cell line, we repeated our assay using recipient MCF-7 cells. MCF-7 cells are human breast adenocarcinoma cells that have been used frequently in studies of drug delivery materials.[59] First, we conducted a control study in which the viability of a confluent monolayer of MCF-7 cells was measured 48 h after free doxorubicin was added directly to the cell media at increasing concentrations from 10 nM to 100 μM (Figure 4j). Next, we exposed independent cell samples to increasing concentrations of Connectosomes, which were equivalent in terms of total doxorubicin content to free doxorubicin concentrations of 180 nM, 900 nM, and 4.5 μM. While the majority of cells treated with Connectosomes at an equivalent doxorubicin concentration of 900 nM was nonviable (61% 7-AAD trypan blue), the majority of cells treated with free doxorubicin remained viable even at a concentration of 100 μM (44% trypan blue), consistent with literature reports[60] (Figure 4j).

As illustrated by these collective results, the therapeutically effective dose (LD50) of doxorubicin increases by more than an order of magnitude when the drug is encapsulated within a conventional liposome, rather than administered to cells as a free drug in solution. This result, which is in agreement with the original literature on liposomal doxorubicin *in vitro*,[16] points to a key limitation of liposomal formulations that has prevented their broad clinical adoption to date. Specifically, their ability to concentrate drugs is largely negated by a corresponding reduction in the availability of the encapsulated drug to the cellular cytoplasm. In contrast, the LD50 for doxorubicin-loaded Connectosomes is more than an order of magnitude less than the LD50 for free doxorubicin and several orders of magnitude less than the LD50 for liposomal doxorubicin. These results illustrate the ability of Connectosomes to dramatically increase the efficiency of drug delivery to the cellular cytoplasm, removing a key limitation of liposomal formulations.[4]

CONCLUSION

Here we report the development of Connectosomes, a cell-derived material that efficiently delivers molecular cargos across the plasma membrane barrier. By utilizing gap junction channels, Connectosomes make it possible to sequester reagents and drugs in a particle, yet release them rapidly and efficiently into the cellular cytoplasm. By combining these two capabilities, Connectosomes represent a key step toward realizing the long-anticipated advantages of particle-based drug delivery materials. In particular, this bioinspired delivery approach has led to a remarkable decrease in the therapeutically effective dose of doxorubicin, which has the potential to address long-standing problems associated with chemotherapy, such as dose-limiting toxicity. Further, this result implies the ability to rapidly increase the drug concentration within the cytoplasm, suggesting the potential to outpace cellular efflux pumps, a key mechanism of multidrug resistance.

The focus of this work has been on fundamental development of Connectosomes as liposomal materials that utilize gap junctions to create a new molecular delivery route to the cytoplasm. However, in the future, these materials could create a path forward for efficient intracellular delivery of hydrophilic drugs and small biologics, including peptides, siRNA, and other compounds with intracellular targets.[31] As evidence of this potential, in Figure 2c, a hydrophilic dye, Atto 594, passed through the connexon channels of Connectosomes. In drug

DOI: 10.1021/jacs.6b05191
J. Am. Chem. Soc. 2016, 138, 12833−12840

design, lack of membrane permeability is currently considered a severe disadvantage that immediately eliminates compounds from drug candidate libraries. However, gap junction-based delivery could remove this requirement, substantially expanding the chemical diversity of drug candidates to include those with high polarity and significant negative charge.[1] For example, this approach could improve the cytoplasmic delivery of drugs that have not been successful in liposomal formulations because they lack membrane permeability, such as cisplatin.[3] Ultimately, by dramatically improving molecular transport across the plasma membrane barrier, Connectosomes have the potential to improve the performance of existing drugs and enable the design of new therapeutics and biochemical reagents that reach a broader class of cytoplasmic targets.

■ ASSOCIATED CONTENT

Supporting Information

The Supporting Information is available free of charge on the ACS Publications website at DOI: 10.1021/jacs.6b05191.

Materials and methods and supporting figures (PDF)

Cell-derived lipid vesicle materials with embedded connexin 43-YFP (AVI)

Donor cells with calcein red-orange (CRO) acetomethoxy (AM) prior to extracting membrane blebs (AVI)

■ AUTHOR INFORMATION

Corresponding Author

*jcstach@austin.utexas.edu

Notes

The authors declare no competing financial interest.

■ ACKNOWLEDGMENTS

We thank Dr. Matthias Falk (Lehigh University) for the generous gift of the connexin 43-YFP cell line. We thank Dr. Janet Zoldan, Dr. Amy Brock, Dr. Laura Suggs, Dr. Subhamoy Das, Dr. Rachel Buchanan, Lindsey Sharpe, and members of the Stachowiak lab (University of Texas at Austin) for valuable feedback on this work. We thank Richard Salinas of the Institute for Cellular and Molecular Biology Core Facility for assistance with flow cytometry. We acknowledge facilities support from Professor Nicholas Peppas and the Institute of Biomaterials, Drug Delivery, and Regenerative Medicine at UT Austin. We acknowledge research funding from the National Science Foundation (DMR1352487 to Stachowiak). A. K. Gadok acknowledges fellowship funding from the National Institutes (T32EB007507).

■ REFERENCES

(1) Lipinski, C. A.; Lombardo, F.; Dominy, B. W.; Feeney, P. J. *Adv. Drug Delivery Rev.* **1997**, *23*, 3−25.

(2) Damaraju, V. L.; et al. *Oncogene* **2003**, *22*, 7524−7536.

(3) Barenholz, Y. *Curr. Opin. Colloid Interface Sci.* **2001**, *6*, 66−77.

(4) Barenholz, Y. *J. Controlled Release* **2012**, *160*, 117−134.

(5) Durand, R. E.; Olive, P. L. *Cancer Res.* **1981**, *41*, 3489−3494.

(6) Ewer, M. S.; Ewer, S. M. *Nat. Rev. Cardiol.* **2015**, *12*, 547−558.

(7) Gottesman, M. M.; Fojo, T.; Bates, S. E. *Nat. rev. Cancer* **2002**, *2*, 48−58.

(8) Overington, J. P.; Al-Lazikani, B.; Hopkins, A. L. *Nat. Rev. Drug Discovery* **2006**, *5*, 993−996.

(9) Mitragotri, S.; Burke, P. A.; Langer, R. *Nat. Rev. Drug Discovery* **2014**, *13*, 655−672.

(10) Phillips, M. A.; Gran, M. L.; Peppas, N. A. *Nano Today* **2010**, *5*, 143−159.

(11) Peer, D.; et al. *Nat. Nanotechnol.* **2007**, *2*, 751−760.

(12) Sahay, G.; Alakhova, D. Y.; Kabanov, A. V. *J. Controlled Release* **2010**, *145*, 182−195.

(13) Thevenin, D.; An, M.; Engelman, D. M. *Chem. Biol.* **2009**, *16*, 754−762.

(14) Yanes, R. E.; et al. *Small* **2013**, *9*, 697−704.

(15) Bareford, L. A.; Swaan, P. W. *Adv. Drug Delivery Rev.* **2007**, *59*, 748−758.

(16) Horowitz, A. T.; Barenholz, Y.; Gabizon, A. A. *Biochim. Biophys. Acta, Biomembr.* **1992**, *1109*, 203−209.

(17) Murthy, N.; Robichaud, J. R.; Tirrell, D. A.; Stayton, P. S.; Hoffman, A. S. *J. Controlled Release* **1999**, *61*, 137−143.

(18) Li, M.; et al. *J. Am. Chem. Soc.* **2015**, *137*, 14084−14093.

(19) Ganta, S.; Devalapally, H.; Shahiwala, A.; Amiji, M. *J. Controlled Release* **2008**, *126*, 187−204.

(20) Mura, S.; Nicolas, J.; Couvreur, P. *Nat. Mater.* **2013**, *12*, 991−1003.

(21) Caldorera-Moore, M.; Guimard, N.; Shi, L.; Roy, K. *Expert Opin. Drug Delivery* **2010**, *7*, 479−495.

(22) Lee, E. S.; Na, K.; Bae, Y. H. *J. Controlled Release* **2005**, *103*, 405−418.

(23) Ashley, C. E.; et al. *Nat. Mater.* **2011**, *10*, 389−397.

(24) Park, J. H.; et al. *Nat. Mater.* **2009**, *8*, 331−336.

(25) Wang, S. G.; et al. *Langmuir* **2013**, *29*, 5030−5036.

(26) Sakhtianchi, R.; et al. *Adv. Colloid Interface Sci.* **2013**, *201−202*, 18−29.

(27) El-Sayed, A.; Futaki, S.; Harashima, H. *AAPS J.* **2009**, *11*, 13−22.

(28) Erazo-Oliveras, A.; Muthukrishnan, N.; Baker, R.; Wang, T. Y.; Pellois, J. P. *Pharmaceuticals* **2012**, *5*, 1177−1209.

(29) Gilleron, J.; et al. *Nat. Biotechnol.* **2013**, *31*, 638−646.

(30) Neijssen, J.; et al. *Nature* **2005**, *434*, 83−88.

(31) Evans, W. H.; Martin, P. E. M. *Mol. Membr. Biol.* **2002**, *19*, 121−136.

(32) Yamasaki, H.; et al. *C. R. Acad. Sci., Ser. III* **1999**, *322*, 151−159.

(33) Huang, R. P.; et al. *Int. J. Cancer* **2001**, *92*, 130−138.

(34) Garcia-Rodriguez, L.; et al. *Mol. Cancer Ther.* **2011**, *10*, 505−517.

(35) Mesnil, M.; Piccoli, C.; Tiraby, G.; Willecke, K.; Yamasaki, H. *Proc. Natl. Acad. Sci. U. S. A.* **1996**, *93*, 1831−1835.

(36) Kaneda, M.; et al. *Biomaterials* **2009**, *30*, 3971−3977.

(37) Charras, G.; Paluch, E. *Nat. Rev. Mol. Cell Biol.* **2008**, *9*, 730−736.

(38) Chen, L.; Novicky, L.; Merzlyakov, M.; Hristov, T.; Hristova, K. *J. Am. Chem. Soc.* **2010**, *132*, 3628−3635.

(39) Costello, D. A.; Hsia, C. Y.; Millet, J. K.; Porri, T.; Daniel, S. *Langmuir* **2013**, *29*, 6409−6419.

(40) Zhao, C.; Busch, D. J.; Vershel, C. P.; Stachowiak, J. C. *Small* **2016**, *12*, 3837−3848.

(41) Simons, M.; Raposo, G. *Curr. Opin. Cell Biol.* **2009**, *21*, 575−581.

(42) EL Andaloussi, E. L. A.; Mager, I.; Breakefield, X. O.; Wood, M. J. *Nat. Rev. Drug Discovery* **2013**, *12*, 347−357.

(43) Sezgin, E.; et al. *Nat. Protoc.* **2012**, *7*, 1042−1051.

(44) Soares, A. R.; et al. *Sci. Rep.* **2015**, *5*, 14888.

(45) Allen, M. J.; Gemel, J.; Beyer, E. C.; Lal, R. *J. Biol. Chem.* **2011**, *286*, 22139−22146.

(46) Thimm, J.; Mechler, A.; Lin, H.; Rhee, S.; Lal, R. *J. Biol. Chem.* **2005**, *280*, 10646−10654.

(47) Muller, D. J.; Hand, G. M.; Engel, A.; Sosinsky, G. E. *EMBO J.* **2002**, *21*, 3598−3607.

(48) Elzarrad, M. K.; et al. *BMC Med.* **2008**, *6*, 20.

(49) Qin, H.; et al. *J. Biol. Chem.* **2002**, *277*, 29132−29138.

(50) Hughes, L. D.; Rawle, R. J.; Boxer, S. G. *PLoS One* **2014**, *9*, e87649.

(51) Preus, D.; Johnson, R.; Sheridan, J.; Meyer, R. *J. Ultrastruct. Res.* **1981**, *77*, 263−276.

(52) Segretain, D.; Falk, M. A. *Biochim. Biophys. Acta, Biomembr.* **2004**, *1662*, 3−21.

DOI: 10.1021/jacs.6b05191
J. Am. Chem. Soc. 2016, 138, 12833−12840

(53) Connors, B. W. *Epilepsy currents/Amer Epilepsy Soc.* **2012**, *12*, 66−68.
(54) Hada, S.; et al. *Oncol. Rep.* **2006**, *16*, 1149−1154.
(55) Maeda, H.; Wu, J.; Sawa, T.; Matsumura, Y.; Hori, K. *J. Controlled Release* **2000**, *65*, 271−284.
(56) Safra, T.; et al. *Ann. Oncology* **2000**, *11*, 1029−1033.
(57) Ohno, S.-i.; et al. *Mol. Ther.* **2013**, *21*, 185−191.
(58) Nurcahyanti, A. D.; Wink, M. *PeerJ* **2016**, *4*, e1542.
(59) Kirpotin, D. B.; et al. *Cancer Res.* **2006**, *66*, 6732−6740.
(60) Kamba, A. S.; Ismail, M.; Ibrahim, T. A.; Zakaria, Z. A.; Gusau, L. H. *BioMed Res. Int.* **2014**, *2014*, 391869.

DOI: 10.1021/jacs.6b05191
J. Am. Chem. Soc. 2016, 138, 12833−12840